



## OPEN Identification of mutations in canine oral mucosal melanomas by exome sequencing and comparison with human melanomas

Maria Lucia Zaidan Dagli<sup>1</sup>✉, Márcia Kazumi Nagamine<sup>1</sup>, Tatícia Lieh Ikeda<sup>1</sup>, Ivone Izabel Mackowiak da Fonseca<sup>1</sup>, Frederico Schmitt Kremer<sup>2</sup>, Fabiana Kommeling Seixas<sup>3</sup>, Carolina Dagli Hernandez<sup>4</sup>, João Vitor Pereira Leite<sup>1</sup>, Cassia Correa Yasumaru<sup>5</sup>, Cristina Oliveira Massoco<sup>5</sup>, Ricardo Hsieh<sup>6</sup>, Silvia Vanessa Lourenço<sup>6</sup> & Tiago Veiras Collares<sup>3</sup>

Oral mucosal melanomas (OMMs) are aggressive neoplasms commonly found in dogs but rare in humans. Utilizing whole exome sequencing (WES), which focuses on protein-coding regions to reveal mutation profiles, we conducted a comparative analysis of canine OMM and human melanomas. This study involved DNA extraction, exome enrichment, and sequencing from three canine OMM cell lines (CMGD-2, CMGD-5, TLM-1), five canine OMM frozen samples, a human OMM cell line (MEMO), and a human commercial skin melanoma cell line (SK-MEL-28). The sequencing and subsequent analysis of FASTQ files yielded final variant files, leading to the identification of mutations. Our findings revealed a total of 500 mutated genes in canine OMM, including significant ones such as EP300, FAT4, JAK3, LRP1B, NCOR1, and NOTCH1. Notably, 82 shared mutations were identified between human melanomas and canine OMM genomes. These mutations were categorized based on the gene functions. The identification of these mutations provides critical insights that can pave the way for the development of novel therapeutic strategies for both canine and human OMM, offering hope for more effective treatments in the future.

**Keywords** Melanoma, Mucosa, Exome sequencing, Mutations, Variants

Mucosal melanoma is a rare and poorly understood subtype of human melanoma and its diagnosis and treatment holds critical importance<sup>1</sup>. Contrarily, canine oral mucosal melanoma (OMM) is the most prevalent oral cancer in dogs, characterized by its aggressive nature and marked by infiltration, recurrence, and metastasis to various organs<sup>2,3</sup>. This study endeavors to juxtapose the genomic landscapes of canine and human OMM to discern potential similarities and disparities in their mutation profiles<sup>4,5</sup>. Despite the heightened aggressiveness of canine OMM, it shares notable resemblances with its human counterpart in clinical presentation, histopathological features, and overall biology<sup>3</sup>. Therefore, dogs are a valuable model for scrutinizing tumor development and tailoring treatments<sup>5</sup>. This research extends beyond mere parallels, delving into genetic factors in dogs to glean insights into OMM progression in both species. Moreover, the shared environment between humans and dogs heightens the relevance of canine OMM in identifying risk factors for these diseases and translating findings into innovative diagnostic and therapeutic modalities<sup>4</sup>.

The challenges in treating OMM stem from the absence of predictive models that faithfully replicate its pathogenesis and molecular alterations<sup>6</sup>. Canine oral melanoma is considered a good model for non-UV melanomas<sup>7</sup>. Addressing this lacuna necessitates further exploration, with a particular focus on canine OMM, to foster the development of novel, less toxic, and more efficacious treatment strategies for human and canine patients<sup>2</sup>. Notably, the anatomical predilection of canine OMM for the gingiva and upper lip, alongside breed-

<sup>1</sup>Laboratory of Experimental and Comparative Oncology, Department of Pathology, School of Veterinary Medicine and Animal Science, University of São Paulo, São Paulo, SP, Brazil. <sup>2</sup>Omixlab – Laboratory of Bioinformatics, Federal University of Pelotas, Pelotas, RS, Brazil. <sup>3</sup>Laboratory of Cancer Biotechnology, Federal University of Pelotas, Pelotas, RS, Brazil. <sup>4</sup>School of Pharmaceutical Sciences, University of São Paulo, São Paulo, SP, Brazil. <sup>5</sup>Laboratory of Comparative Imuno-Oncology, Department of Pathology, School of Veterinary Medicine and Animal Science, University of São Paulo, São Paulo, SP, Brazil. <sup>6</sup>School of Dentistry, University of São Paulo, São Paulo, SP, Brazil. ✉email: mlzdagli@usp.br

specific predispositions, underscores the role of genetic background in driving this disease<sup>8,9</sup>. These distinctions emphasize the unique position of canine OMM in advancing treatments for both species and delineating its genetic disparities and commonalities with human OMM.

Genetic disparities between canine and human OMMs persist, yet recent studies have begun to illuminate potential parallels and distinctions. The resemblance in somatic mutation profiles suggests overlapping molecular pathways between the two species, though variances such as the absence of KIT mutations highlight notable differences<sup>4</sup>. Investigations into metastasis-associated gene expression patterns and transcriptome analyses reveal significant similarities in genetic alterations, tumor location, and histology, particularly between canine and human mucosal melanomas<sup>8,10,11</sup>.

Whole exome sequencing, a targeted genomic method focusing on protein-coding regions, offers a detailed glimpse into mutation profiles, potentially uncovering key driver mutations and therapeutic targets<sup>12,13</sup>. This approach, less expensive than whole-genome sequencing, has been instrumental in diagnosing genetic diseases and gaining insights into the genetic drivers of tumor formation, as demonstrated in recent studies of human oral melanoma<sup>14,15</sup>. Notably, recurrent mutations identified in human oral melanomas, such as those in *KIT*, *POLE*, and *PTCHD2*, signify distinct genetic backgrounds for this malignancy. Similarly, in dogs, whole exome sequencing has proven effective in identifying disease-causing mutations, underscoring its potential utility in comprehensively analyzing the mutation profiles of canine and human OMMs<sup>16</sup>. Thus, herein, we aimed to comprehensively analyze the mutation profiles of canine and human OMMs by performing whole exome sequencing.

## Methods ethics

The experimental procedures were approved by the Committee of Ethics on the Use of Animals (CEUA) of the School of Veterinary Medicine and Animal Science, University of São Paulo (USP), process CEUAx number 5631220119.

## Canine and human melanoma cell lines

Three canine oral melanoma cell lines, CMGD-2, CMGD-5, and TLM-1, with authentication certificates, were purchased from Kerastat (Kerastat Inc., Boston, MA, USA). CMGD-2 is a canine melanoma cell line derived from an oral tumor of a 13-year old castrated male mix breed dog. CMGD5 is a canine melanoma cell line derived from an oral tumor of a 13-year old castrated male miniature poodle. TLM-1 is a canine melanoma cell line derived from an oral tumor of a 12-year old male Gordon setter.

The human oral melanoma cell line, MEMO, was kindly provided by Prof. Silvia Lourenço<sup>1</sup>; it was obtained from a 75 years old male patient, that reported a slow-growing (7 years) black lesion in the hard palate. The human cutaneous melanoma commercial cell line, SK-MEL-28, was purchased from “Banco de Células do Rio de Janeiro” (<https://bcrc.org.br/>); these are neoplastic melanocytes isolated from the skin tissue of a 51-year-old, male patient with malignant melanoma.

## Demographics of the frozen samples of canine OMM

Five frozen samples of canine melanotic OMM samples, named M5, M12, M16, M38, and M41, were kindly provided by Drs. Cristina Oliveira Massoco and Dr Cassia Yasumaru from the Department of Pathology of the School of Veterinary Medicine and Animal Science of the University of São Paulo (SVMAS/USP). All canine OMM were melanotic, and the patient demographics are shown in Table 1.

Immediately after surgical resection, the tumor samples were placed in the Roswell Park Memorial Institute (RPMI) medium until arrival at the laboratory. The samples were fixed in commercial formalin, followed by freezing and storage in a -80°C freezer.

## DNA extraction from the melanoma lines CMGD-2, CMGD-5, TLM-1, MEMO and SK-MEL-28

For extraction, QIAGEN DNeasy Mini Kit (Hilden, Germany) was used according to the manufacturer’s instructions. The cells were cultivated in a monolayer at a concentration of  $5 \times 10^6$  cells per T75 bottle, containing 8 mL of high-glucose Dulbecco’s Modified Eagles Medium with 10% fetal bovine serum and 1% antibiotic-antimycotic agents. After reaching 80% confluence, the cells were trypsinized, and the cell pellet was collected by centrifugation at  $300 \times g$  for 5 min. The supernatant was discarded, and the cell pellet was transferred to a 1.5-mL microtube and eluted in 200  $\mu$ L of AL buffer. Then, 20  $\mu$ L of proteinase K was added. Subsequently, the samples were incubated at 56°C for 10 min. After incubation, the tubes were briefly centrifuged to remove the drops from the lid. A total of 200  $\mu$ L of absolute ethanol was added to the samples, followed by pulse-vortex agitation for 15 s. The samples were centrifuged briefly to remove any solution from the lid. The final solution was carefully applied to the QIAamp Mini centrifuge column (supported by a collection tube).

Code	Breed	Age (years)	Sex	Histological type	Localization	Survival (months)	Clinical Stage
M5	Mongrel	19	F	Epithelioid	gum	1 (30 days)	2
M12	Rottweiler	9	F	Epithelioid	gum	5	3
M16	Cocker spaniel	14	M	Mixed	upper lip	2	2
M38	Mongrel	14	F	Mixed	gum	15 days	3
M41	Maltese	10	F	Spindle	soft palate	5	4

**Table 1.** Demographics of the five canine patients bearing oral mucosal melanoma.

The column was then closed and centrifuged at  $6000 \times g$  for 1 min; it was then transferred to a new 2-mL microcollection tube, and 500  $\mu\text{L}$  of AW1 buffer was added. Centrifugation was performed at  $6000 \times g$  for 1 min. The column was transferred to a new 2-mL microtube, and 500  $\mu\text{L}$  of AW2 buffer was added, followed by centrifugation at  $20,000 \times g$  for 3 min. After changing the microtube again and drying the column by centrifugation, 200  $\mu\text{L}$  of AE buffer was added to the top of the column, followed by incubation at  $15\text{--}25^\circ\text{C}$  for 1 min and centrifugation at  $6000 \times g$  for 1 min.

After DNA extraction, the samples were quantified using the NanoDrop<sup>TM</sup> 2000/2000c spectrophotometer with integrated software (Thermo Fischer Scientific, Waltham, USA). The blank was measured using 1  $\mu\text{L}$  of MilliQ water, whereas the DNA concentration was determined using 1  $\mu\text{L}$  of the sample. Samples with a spectrometry ratio (260/280 nm) of  $2 \pm 0.15$  were used for further experiments. DNA obtained was stored in a  $-70^\circ\text{C}$  freezer.

### DNA extraction from the canine OMM samples

For DNA extraction, DNeasy Tissue and Blood<sup>®</sup> Kit (Qiagen, Hilden, Germany) was used according to the manufacturer's protocol. The samples were thawed, and a small  $1\text{-cm}^2$  piece was removed from each tumor for DNA extraction. The tumor samples were fragmented and placed in a 1.5-mL microtube with 180  $\mu\text{L}$  of ATL buffer and 25  $\mu\text{L}$  of proteinase K. The fragments were incubated at  $56^\circ\text{C}$  until the complete digestion of the tissue (1–3 h). Then, 200  $\mu\text{L}$  of 100% ethanol and 200  $\mu\text{L}$  of AL buffer were added. After brief vortexing, the samples were transferred to QiAmp columns and centrifuged for 1 min at  $6000 \times g$ . The collection tube containing the filtered liquid was discarded, and the column was inserted into a new tube. Then, 500  $\mu\text{L}$  of AW1 was added, followed by centrifugation for 1 min at  $6000 \times g$ . The collection tube containing the filtered liquid was discarded, and the column was inserted into a new collection tube. A total of 500  $\mu\text{L}$  of AW2 was added, followed by centrifugation for 3.5 min at  $20,000 \times g$ . The collection tube was discarded again, and the column was inserted into a new 1.5-mL tube. A second centrifugation step was performed at  $20,000 \times g$  for a minute to dry the column. Then, 200  $\mu\text{L}$  of AE eluent was added to the Qiamp column, and the samples were incubated at room temperature for 1 min, followed by centrifugation at  $6000 \times g$  for 1 min.

After DNA extraction, the samples were quantified using the NanoDrop<sup>TM</sup> 2000/2000c spectrophotometer with integrated software (Thermo Fischer Scientific). The blank was measured using 1  $\mu\text{L}$  of MilliQ water, and the DNA concentration was determined using 1  $\mu\text{L}$  of the sample. Samples with a spectrometry ratio (260/280 nm) of  $2 \pm 0.15$  were used for further analysis.

### Preparation and sequencing of exome libraries

**Sample Quality Check:** DNA integrity was assessed using the Agilent Bioanalyzer 2100 to ensure suitability for further analysis. **DNA Quantification and Library Preparation:** DNA samples were quantified with the Qubit 4 Fluorometer to confirm they met the minimum mass for library preparation. The Illumina Nextera Exome Kit (20020616) was used, requiring 200 ng of genomic DNA in up to 50  $\mu\text{L}$  of ultrapure water. Samples not meeting this requirement were replaced. **Sequencing:** Prepared libraries were analyzed with the Agilent Bioanalyzer 2100 and quantified with the Qubit and KAPA Fast Universal quantitative PCR. Libraries were pooled and clustered on a c-Bot Illumina flow-cell, then sequenced on the HiSeq 2500 platform using Paired-End 2x100 bp v4 chemistry across 4 lanes. **Coverage:** Each lane generated 35 to 40 Gb of data, divided among the libraries (multiplexed), yielding an expected coverage of 6.3 to 7.2 Gb per library. The Nextera DNA Exome kit targets 45 Mb of exonic content, with expected coverage per sample ranging from 140X to 160X.

### Exome enrichment and sequencing workflow

The Nextera DNA Flex Exome Enrichment Kit (Illumina, San Diego, CA, USA) was employed to enrich exomes from canine genomic DNA samples. Although originally designed for human exome enrichment, this kit has been validated for use with canine samples, as demonstrated in the study “Capture of the Canine Exome Using the Nextera Exome Enrichment Kit” by the Animal Health Trust (United Kingdom)<sup>17</sup>.

After enrichment, the captured libraries were quantified and pooled for sequencing using the NextSeq system (Illumina, San Diego, USA). The raw sequencing data (FASTQ files) were then processed to identify gene variants, as illustrated in Fig. 1.

The data analysis workflow included:

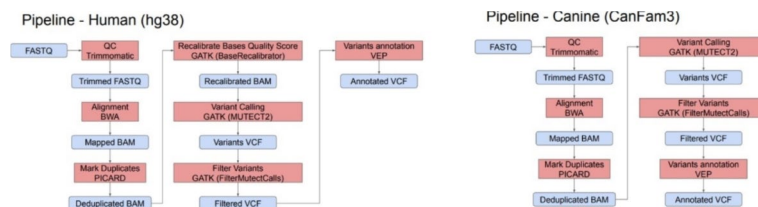


**Fig. 1.** Pipelines used for the preparation of human (a) and canine (b) OMM samples for exome sequencing analysis and identification of mutations. Human melanoma cell lines (MEMO and SK-MEL-128) sequencings were compared to the reference genome hg38, while the canine OMM samples and cell lines sequencings were compared with the CanFam3 reference genome. Details of programs used for the analysis can be found in the text.

- Trim Analysis: Performed using Trimmomatic v0.36–5 to remove low-quality sequences and adapters.
- Read Alignment: Reads were aligned to the canine reference genome (CamFam3) and human genome (hg38) using BWA v0.7.17-r1188.
- Duplicate Identification: Duplicates were marked using the Mark Duplicates tool in Picard v2.26.10.
- Variant Calling: Conducted with MuTect2 (GATK 4.2.5.0).
- Variant Annotation: Performed using Ensembl VEP v102.

The numbers of reads per sample can be seen in Table 2.

## Results

### Canine oral melanomas

The analysis of the whole exome sequencing of the three cell lines and five canine melanoma samples showed 61,267 somatic variants already described in the Ensembl Project database (ensembl.org), with 225 of them having a high impact (0.3%) and 9,327 having a moderate impact (15.2%). Additionally, 957 novel high-impact variants were found and were not cataloged by Ensembl.

Among the variant class types, 92.75% ( $\pm 0.54\%$  standard deviation) were classified as SNV, whereas insertions and deletions accounted for 2.59% ( $\pm 0.58\%$ ) and 2.55% ( $\pm 0.56\%$ ), respectively. The distribution of the variant class types is presented in Fig. 2a.

The most prevalent base changes were G > A (14.54%  $\pm 1.31$ ) and C > T (14.5%  $\pm 1.11$ ), followed by A > G (13.9%  $\pm 0.75$ ), T > C (13.0%  $\pm 0.58$ ), C > A (10.71%  $\pm 1.79$ ), and G > T (10.54%  $\pm 1.64$ ) (Fig. 2b).

Concerning variants affecting protein coding, 58.17% ( $\pm 8.02\%$ ) of the variants were synonymous, with the lowest rate observed in sample M38 (52.8%) and the highest rate observed in the CMGD-5 lineage (77.6%) (Fig. 2c). Non-synonymous variants (missense mutations) accounted for 35.48% ( $\pm 7.23\%$ ), whereas variants with changes in reading frames (frameshift mutations) accounted for 3.36% ( $\pm 1.23$ ) of the total variants.

Additionally, small percentages of insertion (0.63%  $\pm 0.12$ ), deletion (1.19%  $\pm 0.65$ ), and stop-gained variants (1.16%  $\pm 0.44$ ) were observed.

### Human melanomas

For human melanoma samples, 2,084 variants were identified in MEMO, and 3,697 variants were identified in SK-MEL-28. These variants included only the ones already documented in the Ensembl Project database. Upon filtering based on the impact of these variants, MEMO exhibited 26 high-impact variants (1.25%) and 769 moderate-impact variants (29.17%). Notably, 608 high-impact variants and 7,242 moderate-impact variants were newly identified. In the SK-MEL-28 lineage, four high-impact (0.11%) and 337 moderate-impact (9.12%) variants were observed. Additionally, 147 new high-impact and 2,082 new moderate-impact variants were identified in this lineage.

According to the class of variants, SNV-type changes were the most prevalent in both subtypes of human melanoma, with 99.18% in the MEMO and 93.43% in the SK-MEL lineages (Fig. 3).

The most frequent nucleotide base exchanges for the MEMO lineage were C > A (21.94%) and G > T (20.54%), followed by C > T (10.6%) and G > A (10.46%). Conversely, the SK-MEL lineage exhibited a higher frequency of base exchanges with G > A (15.86%) and C > T (14.49%), followed by T > C (13.01%) and A > G (12.24%) (Fig. 4).

Additionally, the SK-MEL lineage showed a higher rate of variants classified as substitutions (3.76%), deletions (1.72%), and insertions (0.96%) than the MEMO lineage.

Synonymous variants accounted for 28.6% and 79.5% of the MEMO and SK-MEL-28 lineages, respectively. Non-synonymous variants (missense mutations) accounted for 65.3% and 18.3% of the MEMO and SK-MEL-28 lines, respectively (Fig. 5). Notably, a pronounced difference between the two human lineages was observed for stop-gained variants, with the MEMO lineage showing 4.2% compared with 0.2% in the SK-MEL-28 lineage. However, the two human lineages showed similar distributions of frameshift variants, insertions, and deletions.

Samples	Number of reads
CMGD-2	79.632.746
CMGD-5	47.379.952
TLM-1	33.573.728
M12	87.015.234
M16	68.344.660
M41	66.859.678
M5	88.546.184
M38	80.774.092
SK-MEL-28	106.816.088
MEMO	44.829.346

**Table 2.** Number of reads per sample.

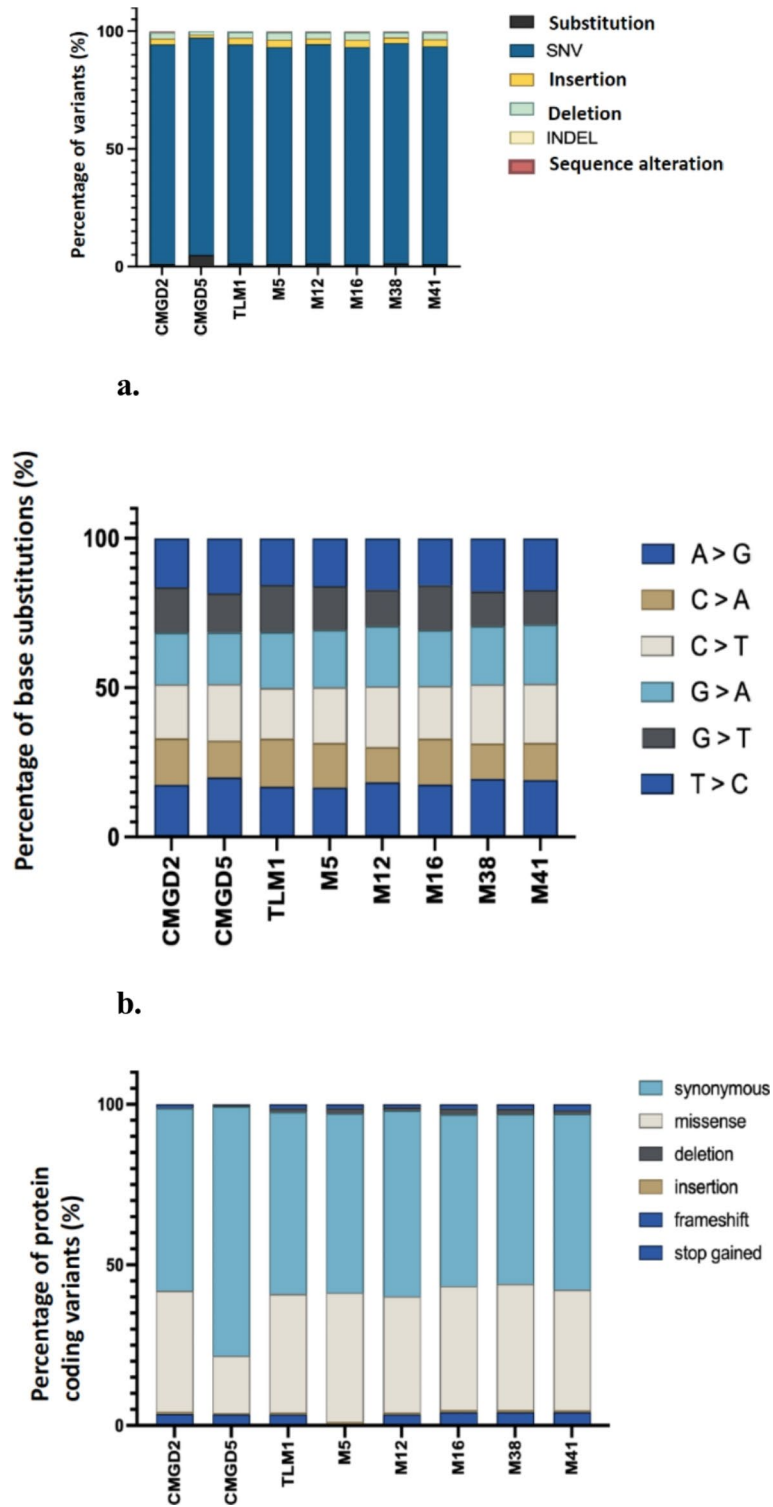


**Fig. 2.** (a) Distribution of different classes of variants among canine oral melanoma lineages; (b) Distribution of single nucleotide substitutions. The graph shows the prevalence of the six most common types of base exchanges in various strains of canine oral melanomas, encompassing high- and moderate-impact variants; (c) Distribution of different variants in protein-coding regions according to canine oral melanoma samples.

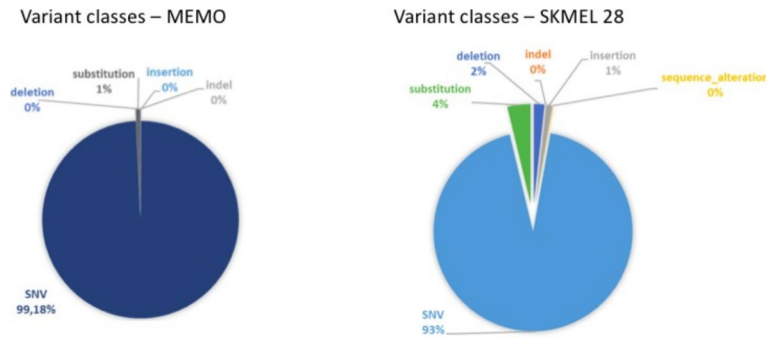


**Fig. 3.** Distribution of different classes of variants among human melanoma cell lines, MEMO and SK-MEL-28.

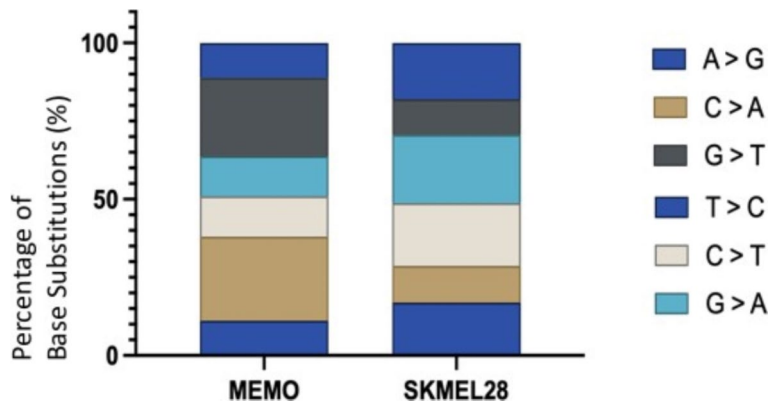


**Fig. 4.** Distribution of single nucleotide substitutions. The graph shows the distribution of the six most prevalent types of base exchanges in different human melanoma lineages.

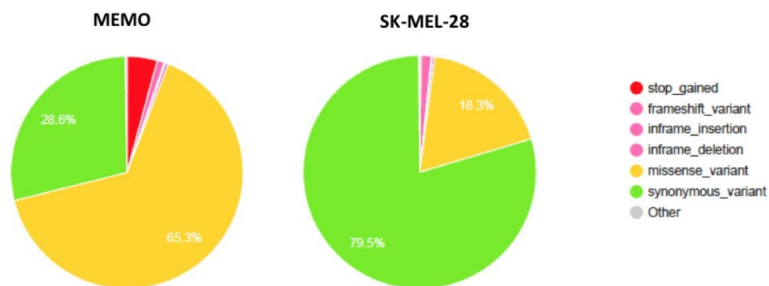


**Fig. 5.** Distribution of different variants in protein-coding regions according to human melanoma samples.

**Comparison of the different classes of variants in canine and human lineages and samples**

The distribution of different classes of variants in canine and human melanoma lineages and samples is found in Table 3.

**Analysis of canine variants in genes involved in oncogenesis**

To identify potential driver mutations involved in oncogenesis, the Catalog of Somatic Mutations in Cancer (COSMIC) was used to search for genes harboring moderate- and high-impact variants in canine oral melanoma samples. Using the cancer gene census list (Cancer Gene Census, v97, tier 1, 578 genes), 500 genes with various variant types were identified across all canine melanoma samples. Among these, 226 genes carried high- and/or moderate-impact variants across different canine lineages. Notably, variants were observed in *EP300*, *FAT4*, *JAK3*, *LRP1B*, *NCOR1*, and *NOTCH1* in all canine samples. The list of the 50 most prevalent genes with changes is presented in Fig. 6.

Sample	Deletion sequence		Indel		Insertion		Alteration		SNV		Substitution		Total	
	QTD	%*	QTD	%*	QTD	%*	QTD	%*	QTD	%*	QTD	%*	QTD	%**
CMGD-2	854	2.49%	26	0.08%	899	2.62%	166	0.48%	31,931	93.13%	409	1.19%	34,285	12.33%
CMGD-5	204	1.41%	1	0.01%	184	1.27%	3	0.02%	13,346	92.33%	716	4.95%	14,454	5.20%
TLM-1	499	2.63%	4	0.02%	536	2.82%	33	0.17%	17,668	93.08%	241	1.27%	18,981	6.83%
M12	971	3.13%	12	0.04%	953	3.07%	141	0.45%	28,542	92.09%	374	1.21%	30,993	11.15%
M16	780	2.53%	21	0.07%	803	2.61%	124	0.40%	28,672	1.28%	30793	11.08%	30793	11.08%
M41	928	3.17%	22	0.08%	874	2.98%	125	0.43%	27,035	1.09%	29303	10.54%	29303	10.54%
M5	738	2.22%	20	0.06%	803	2.41%	120	0.36%	31,172	1.38%	33314	11.98%	33314	11.98%
M38	952	2.86%	27	0.08%	985	2.96%	177	0.53%	30,778	1.14%	33297	11.98%	33297	11.98%
MEMO	23	0.08%	1	0.00%	1	0.00%	0	0.00%	28,314	0.73%	28548	10.27%	28548	10.27%
SK-MEL-28	413	1.72%	9	0.04%	230	0.96%	23	0.10%	22,423	3.76%	24001	8.63%	24001	8.63%

**Table 3.** Distribution of different classes of variants in canine and human melanoma lineages and samples. \*Percentage within each sample. \*\*Percentage of the general total of samples.

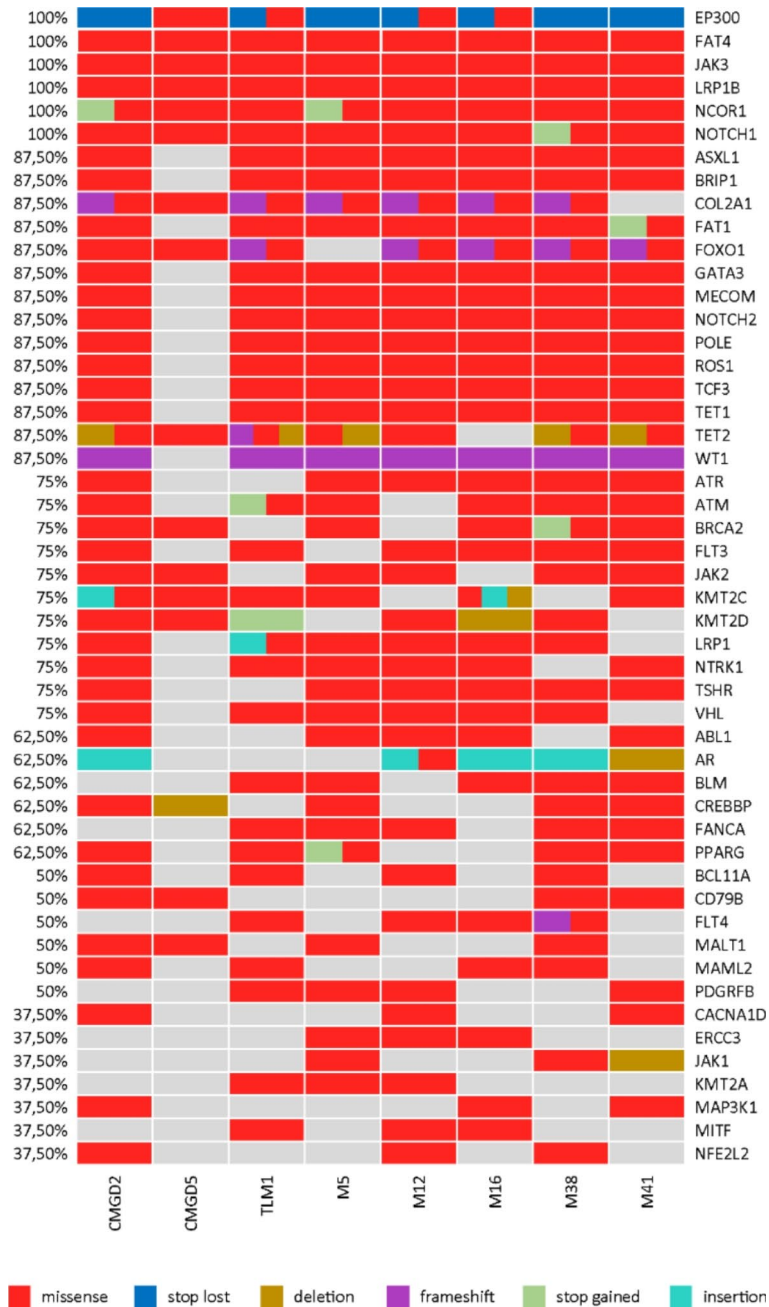


**Fig. 6.** Oncoplot of cancer-related variants in canine OMM, including CMGD2m CMGD5, TLM1, M5, M12, M16, M38 and M41, showing the 50 most prevalent genes with changes.

Tumor sample M5 exhibited the highest number of high- and moderate-impact variants in the genes listed in the COSMIC census (60 genes), followed by the samples M12 and M41, both with 55 affected genes. Conversely, the CMGD-5 lineage showed the lowest number of changes in these genes.

Among the canine OMM samples included in this study, three were from mongrel or mixed-breed dogs (CMGD2, M5, and M38), while five samples (CMGD5, TLM1, M12, M16, and M41) were from purebred dogs. When comparing the two groups (mixed-breed versus purebred), no visible differences in gene alterations were observed in the Oncoplot (Fig. 6).

### Comparative analysis of canine and human oral melanoma samples

A similarity search was performed to identify regions in the canine genome that were homologous to the mutated sites in the human genome. Subsequently, genes located in these syntenic regions in human and canine genomes were selected, and mutations in these regions were extracted from the VCF files. Shared mutations were identified between the two species, representing genes mutated in melanoma samples from humans and dogs. Initially, 131 mutated genes were found in all the samples from both the species. Subsequently, a new filtering



process was implemented to eliminate duplicate genes, which resulted in a refined list of 82 mutated genes common between human and canine melanomas (Tables 4, 5). Mutated genes were categorized according to their common function using the NCBI website (<https://www.ncbi.nlm.nih.gov/guide/howto/find-func-gene/>) and other references. The categories were: Ion channels and transporters, receptors and signaling proteins, structural and cytoskeleton proteins, transcription factors and regulatory proteins, cell adhesion and extracellular proteins, RNA processing and regulation, signaling and regulatory proteins, apoptosis and cell cycle regulation, and other functions.

In addition, the genes with shared mutations in canine and human OMM samples involved in signal transduction were identified using the Reactome Knowledgebase (Reactome: <https://pubmed.ncbi.nlm.nih.gov/34788843/>)

Figure 7 shows the heatmap of mutation profile among genes in melanomas with homologs in both dogs and humans. This heatmap shows all genes that had at least 1 mutation identified in canine or human OMM and SK-MEL-28 cells. The CMGD5 sample, a canine OMM cell line, showed the highest level of mutations than the other samples. The MEMO, a human OMM cell line, presented the lowest level of mutations shared with dogs.

## Discussion

Canine oral melanoma is an extremely aggressive and mutilating neoplasm, and is marred by limited treatment options<sup>19</sup>. Canine OMM accounts for 30–40% of oral tumors in dogs. It predominantly occurs in older dogs, especially certain breeds like Cocker Spaniels, Poodles, and Golden Retrievers. Canine OMM is characterized by rapid progression, high metastatic potential, and poor prognosis, with median survival times ranging from months to over a year<sup>19</sup>.

In humans, mucosal melanoma is a rare and aggressive subtype that contrasts with its cutaneous counterpart; it occurs more frequently in males between 41–60 years old, and the innovative treatment approaches against it offer limited benefits. These limitations are attributed to the scarcity of actionable driver mutations and poor response to immunotherapy<sup>11</sup>. However, the application of whole-genome and exome sequencing techniques has significantly contributed to advancing the understanding of the molecular landscape of mucosal melanoma<sup>11,14–16</sup>.

The exome is a fraction of the genome and should cover the vast majority of the protein coding genes; it is crucial for understanding genetic variations. The human genome consists of a string of 3 billion bases (A, T, C, and G), with genes accounting for only 1–2% of the total genome, accounting for a string of approximately 30–60 million bases. Exons, which code for amino acids in each gene, constitute the protein-coding regions of the genome, thus the name exome. Whole exome sequencing (WES) enables the direct assessment of these protein-coding regions<sup>12</sup>. Consequently, researchers and physicians are increasingly using exome sequencing to diagnose genetic diseases.

In humans, several studies have undertaken comprehensive sequencing analyses to understand the molecular landscape of human OMM. In a groundbreaking study, researchers recently performed WES on 19 samples of human oral melanomas, correlating tumor samples with normal tissues, to gain insights into the potential genetic drivers of tumor formation<sup>14</sup>. Lyu et al.<sup>14</sup> identified recurrent alterations in genes like BRAF, NRAS, KIT, and GNAQ/GNA11, with 55% of tumors harboring MAPK pathway mutations. Newell et al.<sup>15</sup> performed exome sequencing in human OMM and this technique has proven successful in identifying disease-causing mutations and dominant and recessive Mendelian disorders

In another study, Indini et al.<sup>11</sup> reviewed the literature, highlighting BRAF, NRAS, KIT, and NF1 as the most commonly mutated genes in mucosal melanomas. Hsieh et al.<sup>20</sup> observed NRAS mutations were more common than BRAF mutations in primary oral mucosal melanomas.

The increased mutational burden of melanoma tumors and the consequent high load of neoantigens in these tumors may contribute to the greater efficacy of immunotherapies<sup>21</sup>. Mutanome analysis can be used as a tool to identify therapeutic targets in different cancer types<sup>22–24</sup>. In this context, identifying such targets through the mapping of the oral melanoma mutanome can significantly contribute to developing new therapies against this specific cancer type. Several studies involving exome sequencing have been performed on human neoplasms<sup>14,15,25–29</sup>; however, only a few studies are available on canine oral melanoma<sup>30,31</sup>. Therefore, herein, we aimed to detect mutations in canine oral melanomas with the potential to provide insights into the development of new therapies for this aggressive neoplasm.

Herein, we analyzed eight canine oral melanoma samples, comprising five oral melanoma samples and three lineages, in addition to two samples of human melanomas, one oral melanoma sample (MEMO lineage), and one cutaneous melanoma sample (SK-MEL-28). Exome sequencing revealed similar variant patterns in the canine samples, including the class distribution of single-nucleotide mutations and changes in protein-coding regions. No visible differences were detected when OMM in mixed breed dogs and purebred dogs were compared. Notably, the CMGD-5 lineage exhibited pronounced differences, exhibiting a higher rate of substitution variants and a greater prevalence of synonymous variants than those in other canine lineages. Additionally, it exhibited the highest number of changes in genes listed in the COSMIC database. These results are consistent with the findings in other canine tumor lineages<sup>32</sup>. Conversely, the human lineages exhibited differences in several aspects of the mutations given their distinct subtypes. These differences are consistent with previously reported etiologies, risk factors, and mutation patterns in different melanoma subtypes<sup>33</sup>.

It was interesting and surprising to see that 82 genes have shown alterations in both canine and human melanoma samples.

The evaluation of possible driver mutations revealed that five genes presented high- and/or moderate-impact variants in all canine lineages. Four of these genes (*EP300*, *FAT4*, *LRP1B*, and *NCOR1*) were identified as tumor suppressor genes (TSGs), *JAK3* was classified as an oncogene, and *NOTCH1* was described as both a TSG and an oncogene. Additionally, changes in *LRP1B* were prevalent in various tumor cell lines studied by Das et al.

Gene names	Gene function	Mutations in human OMM	Mutations in canine OMM
<b>Ion channels and transporters</b>			
<i>ATP2B2</i>	Calcium pump that regulates intracellular calcium levels	chr3:g.10326098_10326099insC A;3:g.10402143G > C;3:g.10338242G > A	chr20:g.8025625A > G
<i>CACNA1F</i>	Voltage-dependent calcium channel involved in neurotransmitter release	chrX:g.49210308 T > C	chrX:g.42319214 T > C;X:g.4231 4144C > A;X:g.42314055_42314056insGT;X:g.42314036A > G; X:g.42314067_42314068del
<i>KCNF1</i>	Potassium channel involved in neuronal excitability	chr2:g.10913614C > T	chr17:g.7753742 T > C
<i>KCNH3</i>	Potassium channel that affects cardiac action potentials	chr12:g.49544030A > G	chr27:g.5079930 T > C
<i>KCNK3</i>	Inwardly rectifying potassium channel involved in setting the resting membrane potential	chr2:g.26728322G > C	chr17:g.20732996 T > G;17:g.20733014C > G;17:g.20732911C > G;17:g.20732905G > C;17:g.20732927C > G
<i>KCNQ1</i>	Potassium channel critical for cardiac repolarization	chr11:g.2673646A > T;11:g.2652 345G > A;11:g.2681283C > T;11:g.0.2683945A > G	chr18:g.46658512 T > C
<i>Orai3</i>	Calcium release-activated calcium channel involved in immune response	chr16:g.30953619A > G	chr6:g.17450354 T > C
<i>SCN5A</i>	Sodium channel critical for action potentials in cardiac tissue	chr3:g.38548175_38548176insT CCCTCCTTTTCTACTCTC TTCTC	chr23:g.8337283A > G
<i>CACNB3</i>	Auxiliary subunit of voltage-gated calcium channels	chr12:g.48825720 T > C	chr27:g.5714410C > A;27:g.571 4405G > C
<i>TRPM7</i>	Ion channel and kinase involved in magnesium homeostasis	15:g.50611285C > T	chr30:g.16579822A > G;30:g.1 6579709A > G
<i>SLC4A3</i>	An anion exchanger that helps regulate intracellular pH and ion balance	chr2:g.219629396A > C	chr37:g.26144825 T > C
<i>ABCC12</i>	is part of the ATP-binding cassette (ABC) transporter family, involved in the transport of various molecules across cellular membranes	chr16:g.48100945 T > A	chr2:g.66938684 T > A;2:g.6693 8679A > C;2:g.66938698_66938699delinsTT;2:g.66938694_66938695del
<b>Receptors and signaling proteins</b>			
<i>ADGRL1</i>	Adhesion G protein-coupled receptor involved in neuronal development	chr19:g.14149951C > T	chr20:g.48420263A > G;20:g.4 8523793A > G
<i>CHRNA4</i>	Nicotinic acetylcholine receptor involved in neurotransmission	chr20:g.63346079C > T;20:g.633 61195G > C;20:g.63350733A > G;20:g.63350772A > G	chr24:g.47080007G > T;24:g.47 080001A > G;24:g.47080004
<i>FLT1</i>	Vascular endothelial growth factor receptor involved in angiogenesis	chr13:g.28387702C > T	chr25:g.11330040G > T;25:g.11 330154_11330155del;25:g.11330099 T > A;25:g.11330151_11330152delinsGC;25:g.11330102_11330103del
<i>GPR137 (or BAD)</i>	G protein-coupled receptor implicated in various signaling pathways	chr18:g.52816095G > A	chr18:g.52816095G > A
<i>JAK3</i>	Janus kinase involved in cytokine signaling	chr19:g.17847968 T > C	chr20:g.45054061A > G
<i>OPRK1</i>	Opioid receptor involved in pain modulation	chr8:g.53226041A > T;8:g.532260 58G > T;8:g.53226301 T > C;8:g.53228388C > T;8:g.53227469C > T;8:g.53225731C > T;8:g.53226489G > C;8:g.53228439G > A;8:g.53226496A > G	chr29:g.5051663G > C
<b>Structural and cytoskeletal proteins</b>			
<i>CAMSAP2</i>	Mic otubule-associated protein involved in cytoskeletal organization	chr1:g.200858053G > A	chr7:g.2320447C > T
<i>DCC</i>	Netrin receptor involved in axon guidance	chr18:g.53322129 T > A	chr1:g.21862860 T > C;1:g.21918 555A > G;1:g.21952313G > A
<i>DNAH12</i>	Dynein heavy chain involved in ciliary movement	chr3:g.57433770C > T	chr20:g.32985652G > A
Continued			

Gene names	Gene function	Mutations in human OMM	Mutations in canine OMM
<i>HSPG2</i>	Heparan sulfate proteoglycan involved in cell adhesion and signaling	chr1:g.21880449G > A	chr2:g.77359228_77359230del; 2:g.77359226_77359227insCC G; 2:g.77359227 T > G
<i>KRT13</i>	Keratin involved in structural integrity of epithelial cells	chr17:g.41502942 T > C	chr9:g.21261775 T > C
<i>KRT36</i>	Keratin involved in structural integrity of epithelial cells	chr17:g.41489769A > G	chr9:g.21280103 T > C
<i>KRT6B</i>	Keratin involved in structural integrity of epithelial cells	chr12:g.52447900C > G	chr27:g.2596103 T > C
<i>KRT71</i>	Keratin involved in structural integrity of epithelial cells	chr12:g.52552714C > T; 12:g.5255 2759C > T	chr27:g.2422632 T > C
<i>KRT76</i>	Keratin involved in structural integrity of epithelial cells	chr12:g.52772156C > T	chr27:g.2422632 T > C
<b>Transcription factors and regulatory protein</b>			
<i>DUSP3</i>	Dual specificity phosphatase involved in MAPK signaling regulation	chr17:g.43769596 T > C	chr9:g.19518812 T > C
<i>EBF2</i>	Transcription factor involved in B-cell development	chr8:g.25850751 T > C	chr25:g.31481727A > C; 25:g.31481736 T > G; 25:g.31481718 T > C; 25:g.31481730C > T; 25:g.31481733C > T; 25:g.31481724C > G; 25:g.31481691 T > C; 25:g.31481 739 T > C
<i>FOXA2</i>	Transcription factor involved in endodermal organ development	chr20:g.22582036 T > C	chr24:g.1012177_1012178delin sTC
<i>MECOM</i>	Transcription factor involved in hematopoiesis and development	chr3:g.169083707C > A	chr34:g.33764534 T > C; 34:g.337 79388A > G
<i>PKD1</i>		chr16:g.2108300G > A	chr6:g.38849682 T > G
<i>PRDM16</i>	Transcription factor involved in brown fat differentiation	chr1:g.3405575C > T	chr5:g.58000768G > C
<i>TCFL5</i>	Transcription factor involved in cell cycle regulation	chr20:g.62841264_62841268del; 20:g.62841244G > A; 20:g.62841456G > C	chr24:g.47080007G > T; 24:g.47 080001A > G; 24:g.47080004_47080005delinsGG; 24:g.4676158 2G > A; 24:g.47000760G > T
<i>ZBTB40</i>	Transcription factor involved in immune response	chr1:g.22520216G > A	chr2:g.76784558 T > C
<i>GATA2</i>	zinc-finger transcription factor that regulates the expression of genes critical for the development, maintenance, and functionality of various blood cell lineages and stem cells	chr3:g.128487775C > A	chr20:g.2474760C > G
<b>Cell adhesion and extracellular matrix</b>			
<i>NID2</i>	Extracellular matrix protein involved in cell adhesion	chr14:g.52011597A > G	chr8:g.28261424 T > C
<i>CSMD2</i>	May be involved in cell-cell adhesion and signaling	chr1:g.33724288G > A; 1:g.335154 18A > T	chr15:g.8040257 T > A; 15:g.804 0246 T > A
<i>CELSR2</i>	Involved in cell adhesion and the regulation of planar cell polarity	chr1:g.109275641G > A; 1:g.10927 1668C > T	chr6:g.42570429G > A
<i>PCDH7</i>	A calcium-dependent cell-adhesion protein that mediates cell-cell interactions	chr4:g.31144993C > T	chr3:g.80388661G > T
<i>EFEMP2</i>	An extracellular matrix protein that may play a role in tissue development and repair	chr11:g.65872733C > T	chr18:g.51392571G > A; 18:g.51 392862G > C
<i>TNN</i>	An extracellular matrix protein involved in structural support	chr1:g.175123571C > T	chr7:g.24257415G > A
Continued			

Gene names	Gene function	Mutations in human OMM	Mutations in canine OMM
<i>ADAMTSL2</i>	A component of the extracellular matrix that plays a role in tissue development and repair	chr9:g.133547133A > C	chr9:g.49954100A > G;9:g.4993 1285 T > C
<i>FLT1</i>	A receptor for vascular endothelial growth factor (VEGF) involved in angiogenesis	chr13:g.28387702C > T	chr25:g.11330040G > T;25:g.11 330154_11330155del;25:g.113 30099 T > A;25:g.11330151_113 30152delinsGC;25:g.11330102_11330103del
<i>KRT6B</i>	A keratin involved in the structural integrity of epithelial cells	chr12:g.52447900C > G	chr27:g.2596103 T > C
<i>KRT71</i>	Another keratin involved in maintaining the structure of epithelial tissues	chr12:g.52552714C > T;12:g.5255 2759C > T	chr27:g.2422632 T > C
<b>RNA processing and regulation</b>			
<i>PABPC1</i>	Poly(A) binding proteins involved in mRNA stability and translation	chr8:g.100717808_100717809ins TC;8:g.100717782 T > C	chr13:g.2564157G > A
<i>PABPC3</i>	Poly(A) binding proteins involved in mRNA stability and translation	chr13:g.25097005A > G;13:g.2509 7062C > T;13:g.25097034C > A;13: g.25097016_25097025del;13:g.2 5096984C > T;13:g.25096877A > G ;13:g.25097072C > T;13:g.250968 70C > T;13:g.25097068A > G;13:g. 25097030C > T;13:g.25097011_25 097014del	chr13:g.2564157G > A
<i>CPSF7</i>	A component of the cleavage and polyadenylation specificity factor complex involved in mRNA processing	chr11:g.61411813G > A	chr18:g.54987464 T > G
<i>NMD3</i>	Involved in nonsense-mediated decay, a quality control mechanism for mRNA	chr3:g.161251480C > T	chr34:g.27231308C > T
<i>PUS10</i>	A pseudouridine synthase involved in tRNA modification	chr2:g.60940865G > T;2:g.609406 26A > G	chr10:g.61100451C > T
<i>TNRC6B</i>	A component of the RNA-induced silencing complex (RISC) involved in gene silencing	chr22:g.40324860_40324862del; 22:g.40327705A > G;22:g.403248 64 T > C	chr10:g.24852007C > A;10:g.24 852011C > A
<i>SMG1</i>	Kinase involved in mRNA surveillance and nonsense-mediated decay	chr16:g.18838206 T > C	chr6:g.26258381C > T
<i>DCLK3</i>	A kinase involved in regulating mRNA translation and stability	chr3:g.36714868_36714869insTC CC;3:g.36714864_36714866del;3 :g.36714870_36714879del	chr23:g.6631170C > T
<b>Signaling and regulatory proteins</b>			
<i>HERC1</i>	An E3 ubiquitin ligase that regulates protein degradation and signaling pathways	chr15:g.63661830C > T	chr30:g.28317368_28317369ins CA;30:g.28317356_28317357d elinsGA
<i>ARHGEF25</i>	A guanine nucleotide exchange factor for Rho GTPases involved in cytoskeletal dynamics	chr12:g.57613448A > G	chr10:g.1793790A > G
<i>DYRK1A</i>	A kinase that regulates various signaling pathways and is implicated in neuronal development	chr21:g.37512973G > T;21:g.3751 2999 T > G	chr31:g.32652221_32652222ins AG
<i>MAPKAP1</i>	Involved in signaling pathways that regulate cell growth and differentiation	chr9:g.125484456G > A	chr9:g.57655456A > G
<i>GALNT2</i>	A glycosyltransferase involved in O-glycosylation of proteins, influencing signaling pathways	chr1:g.230279498 T > C	chr4:g.9058186 T > C
<i>PHIP</i>	A protein that interacts with signaling pathways related to cell growth and survival	chr6:g.78940076_78940077insT AA	chr12:g.39919380A > G
<i>SIX4</i>	A transcription factor involved in developmental processes and signaling pathways	chr14:g.60711061G > A	chr8:g.35736645G > C;8:g.3573 6642A > T
Continued			

Gene names	Gene function	Mutations in human OMM	Mutations in canine OMM
<i>FURIN</i>	A proprotein convertase involved in the processing of various proteins, influencing signaling pathways	chr15:g.90878193C > T	chr3:g.53360659 T > G;3:g.5336 0566 T > G
<i>HADHB</i>	A mitochondrial enzyme involved in fatty acid metabolism and signaling pathways	chr2:g.26254257_26254258insG ACT	chr17:g.20395930G > A
<i>KLC4</i>	A kinesin light chain involved in intracellular transport and signaling	chr6:g.43046560_43046561delins CC	chr12:g.11540386C > T
<b>Apoptosis and cell cycle regulation</b>			
<i>BBC3</i>	Pro-apoptotic gene involved in the regulation of apoptosis	chr19:g.47221435 T > C	chr1:g.108889479 T > C;1:g.1088 89549C > G;1:g.108889541C > G ;1:g.108889504C > A;1:g.10888 9507_108889508delinsAG
<i>TIMP3</i>	An inhibitor of matrix metalloproteinases involved in tissue remodeling and apoptosis	chr22:g.32862301 T > C	chr10:g.30681498G > C
<b>Other functions</b>			
<i>MAP1B</i>	Microtubule-associated protein involved in neuronal development	chr5:g.72207680C > G	chr2:g.55247426A > G
<i>LRCH4</i>	May play a role in cytoskeletal organization and signaling	chr7:g.100577850 T > C	chr6:g.9112365G > C;6:g.91123 35 T > C;6:g.9112337 T > C;6:g.91 12359 T > C;6:g.9112386 T > C;6: g.9112392G > C
<i>MRPL21</i>	A mitochondrial ribosomal protein involved in protein synthesis	chr11:g.68898012 T > C	chr18:g.49088688A > T
<i>CCNT1</i>	A cyclin that regulates transcription elongation and cell cycle progression	chr12:g.48690651G > A;12:g.4869 3697 T > A	chr27:g.5816315_5816316delin sAT;27:g.5816313C > G
<i>CUL9</i>	A component of E3 ubiquitin ligase complexes involved in protein degradation	chr6:g.43188548C > T	chr12:g.11540386C > T
<i>PCNX3</i>	Function is less well characterized but may be involved in cellular processes	chr11:g.65634561C > G	chr18:g.51574377G > A;18:g.51 590933 T > C
<i>TEPP</i>	Function is not well defined	chr16:g.57985492G > A	chr2:g.58570459A > G
<i>ZYG11B</i>	A component of E3 ubiquitin ligase complexes involved in protein regulation	chr1:g.52826935 T > A	chr5:g.56190072 T > C;5:g.56189 515 T > C
<i>GRAMD4</i>	Function is not well defined but may be involved in cellular signaling	chr22:g.46663095 T > C	chr10:g.19606974 T > A
<i>LRRTM2</i>	Involved in synaptic function and neuronal development	chr5:g.138870511G > T;5:g.13887 1844G > A;5:g.138934902_13893 4906del	chr11:g.26391211 T > A;11:g.26 391169_26391170insTAGAA
<i>NCL</i>	A nucleolar protein involved in ribosome biogenesis	chr2:g.231457719 T > C	chr25:g.43331241 T > C
<i>PHKG2</i>	A regulatory subunit of phosphorylase kinase involved in glycogen metabolism	chr16:g.30757171_30757178del	chr6:g.17450354 T > C
<i>POMT2</i>	Involved in protein O-mannosylation	chr14:g.77275634C > T;14:g.7727 5051 T > C;14:g.77275875C > T	chr8:g.50126716 T > A
<i>VSTM2L</i>	Function is less well characterized but may be involved in cellular processes	chr20:g.37944349C > T	chr24:g.26442776 T > G
<i>SSBP2</i>	involved in DNA repair processes and may play a role in regulating transcription	chr5:g.81440625A > G	chr3:g.25900499A > G

**Table 4.** Mutated genes (82 genes) and their chromosome (chr) location in canine and human oral mucosal melanoma categorized according to common function. Please, also see Supplementary Material for further information on individual gene functions.

Signal transduction pathway	Genes
Signaling by receptor tyrosine kinases	FURIN, MAPKAP1, PTPRS, FLT1, DUSP3, JAK3, ITGAV LRRTM2, CHRNA4, KCNQ1, KCNF1, KCNH3, PTPRS,
Signaling by TGF $\beta$ family members	CACNB3, KCNK3, LIN7C
Signaling by GPCR	OPRK1, ARHGEF25
Signaling by NOTCH	NRC6B, FURIN
Signaling by WNT	TNRC6B
Signaling by nuclear receptors	TNRC6B, CCNT1
Signaling by MAPK cascades	JAK3, TNRC6B
Intercellular signaling by second messengers	MAPKAP1, TNRC6B, MECOM
Signaling by Rho GTPases, Miro GTPases and RHOBTB3	PHIP, CPSF7, KLC4, ARHGEF25, PCDH7

**Table 5.** Genes with shared mutations among canine and human melanoma samples related to signal transduction pathways identified using Reactome Knowledgebase (<https://reactome.org/>).

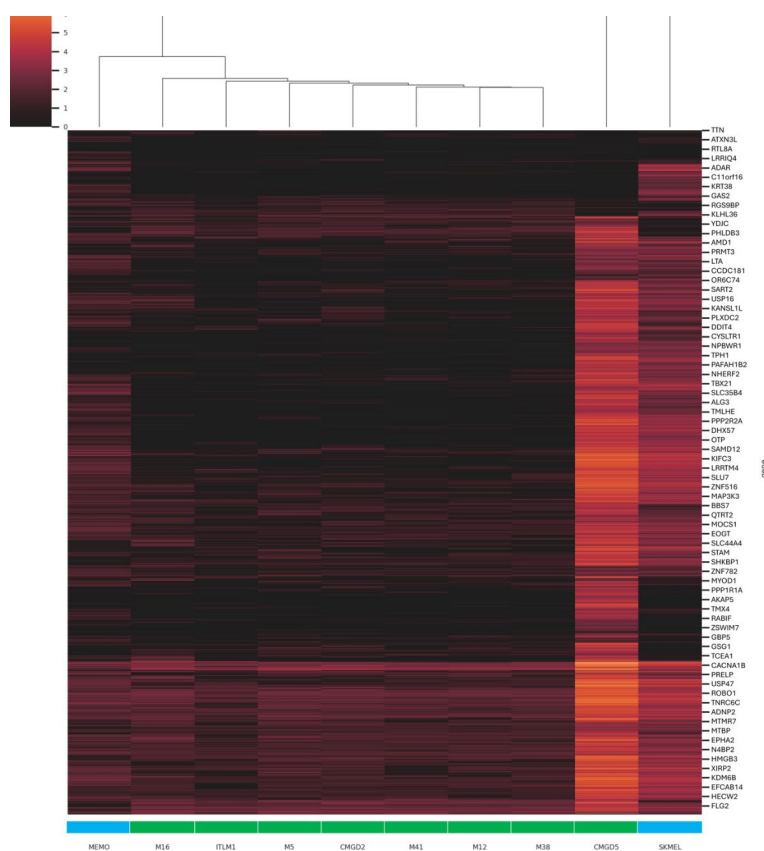


**Fig. 7.** Mutations among genes with homologs in both humans and dogs that exhibited mutations in at least one of the samples. Notably, the CMGD-5 sample showed the highest level of mutations than the other samples. In contrast, the MEMO, a human oral melanoma line, presented the lowest level of mutations. MEMO and SK-MEL-28 are human melanoma cell lines (in blue); TLM-1, CMGD-2 and CMGD-5 are canine oral melanoma cell lines, and M16, M5, M41, M12 and M38 are canine oral melanoma frozen samples (in green).

(2019)<sup>32</sup>, and these genes were featured in the canine cancer gene panel (OncoPanel) developed and validated by Wang et al. in 2021<sup>34</sup>.

The limitations of this study are as follows:

- The study included a limited number of canine oral mucosal melanoma cell lines and samples.
- Two human cell lines were used: one oral mucosal melanoma (OMM) and one skin melanoma (SK-MEL-28). We recognize that a broader inclusion of both human and canine samples is necessary in future studies, as mutations in cancer patients can vary significantly even within the same type of cancer.

- The mutations identified in this study were determined by comparing the sequencing data to reference genomes rather than to germline sequences.

## Conclusions

In this study, mutated genes were identified in three canine OMM cell lines and five canine OMM samples; a total of 500 mutated genes were identified in canine OMM, including significant ones such as EP300, FAT4, JAK3, LRP1B, NCOR1, and NOTCH1. Notably, 82 shared mutations were identified between human melanomas and canine OMM genomes. The identification of these mutations provides critical insights that can pave the way for the development of novel therapeutic strategies for both canine and human OMM, offering hope for more effective treatments in the future. The identification of commonly altered genes in oral melanomas is important in comparative oncology. A list of genes involved in oncogenesis was generated in this study, which provides a basis for identifying potential candidates for gene manipulation and possibly new treatment approaches.

## Data availability

The datasets generated and analyzed during the current study are available in the SRA database under the reference PRJNA1090544 (<https://www.ncbi.nlm.nih.gov/sra/PRJNA1090544>).

Received: 26 February 2024; Accepted: 30 September 2024

Published online: 15 October 2024

## References

- Lourenço, S. V. et al. Establishment and characterization of an oral mucosal melanoma cell line (MEMO) derived from a longstanding primary oral melanoma. *Am. J. Dermatopathol.* **35**, 248–251. <https://doi.org/10.1097/DAD.0b013e31826a9905> (2013).
- Bergman, P. J. Canine oral melanoma. *Clin. Tech. Small. Anim. Pract.* **22**, 55–60. <https://doi.org/10.1053/j.ctsap.2007.03.004> (2007).
- Nishiya, A. T. et al. Comparative aspects of canine melanoma. *Vet. Sci.* **3**, 7. <https://doi.org/10.3390/vetsci3010007> (2016).
- Wong, K. et al. Cross-species genomic landscape comparison of human mucosal melanoma with canine oral and equine melanoma. *Nat. Commun.* **10**, 353. <https://doi.org/10.1038/s41467-018-08081-1> (2019).
- Bongiovanni, L., Brachelente, C., Dow, S. & Bergman, P. J. Editorial: Canine melanoma in comparative oncology: Translate research advances to develop new diagnostic and therapeutic options. *Front. Vet. Sci.* **9**, 1127527. <https://doi.org/10.3389/fvets.2022.1127527> (2023).
- Segaoula, Z. et al. Isolation and characterization of two canine melanoma cell lines: new models for comparative oncology. *BMC Cancer* **18**, 1219. <https://doi.org/10.1186/s12885-018-5114-y> (2018).
- Gillard, M. et al. Naturally occurring melanomas in dogs as models for non-UV pathways of human melanomas. *Pigment Cell Melanoma Res.* **27**(1), 90–102. <https://doi.org/10.1111/pcmr.12170> (2014).
- Hernandez, B. et al. Naturally occurring canine melanoma as a predictive comparative oncology model for human mucosal and other triple wild-type melanomas. *Int. J. Mol. Sci.* **19**, 394. <https://doi.org/10.3390/ijms19020394> (2018).
- Palma, S. D., McConnell, A., Verganti, S. & Starkey, M. Review on canine oral melanoma: An undervalued authentic genetic model of human oral melanoma?. *Vet. Pathol.* **58**, 881–889. <https://doi.org/10.1177/0300985821996658> (2021).
- Simpson, R. M. et al. Sporadic naturally occurring melanoma in dogs as a preclinical model for human melanoma. *Pigment. Cell. Melanoma Res.* **27**, 37–47. <https://doi.org/10.1111/pcmr.12185> (2014).
- Indini, A., Roila, F., Grossi, F., Massi, D. & Mandalà, M. Molecular profiling and novel therapeutic strategies for mucosal melanoma: A comprehensive review. *Int. J. Mol. Sci.* **23**, 147. <https://doi.org/10.3390/ijms23010147> (2021).
- Ng, S. B. et al. Targeted capture and massively parallel sequencing of 12 human exomes. *Nature* **461**, 272–276. <https://doi.org/10.1038/nature08250> (2009).
- Petersen, B. S., Fredrich, B., Hoepfner, M. P., Ellinghaus, D. & Franke, A. Opportunities and challenges of whole-genome and -exome sequencing. *BMC Genet.* **18**, 14. <https://doi.org/10.1186/s12863-017-0479-5> (2017).
- Lyu, J. et al. Whole-exome sequencing of oral mucosal melanoma reveals mutational profile and therapeutic targets. *J. Pathol.* **244**, 358–366. <https://doi.org/10.1002/path.5017> (2018).
- Newell, F. et al. Whole-genome landscape of mucosal melanoma reveals diverse drivers and therapeutic targets. *Nat. Commun.* **10**, 3163. <https://doi.org/10.1038/s41467-019-11107-x> (2019).
- Broeckx, B. J. G. et al. An exome sequencing based approach for genome-wide association studies in the dog. *Sci. Rep.* **7**, 15680. <https://doi.org/10.1038/s41598-017-15947-9> (2017).
- Animal Health Trust [https://www.illumina.com/content/dam/illumina-marketing/documents/products/appnotes/appnote\\_nextera\\_exome\\_enrichment\\_canine.pdf](https://www.illumina.com/content/dam/illumina-marketing/documents/products/appnotes/appnote_nextera_exome_enrichment_canine.pdf)
- Zhang, P. et al. SeqTailor: A user-friendly webserver for the extraction of DNA or protein sequences from next-generation sequencing data. *Nucleic Acids Res.* **47**(W1), W623–W631. <https://doi.org/10.1093/nar/gkz326> (2019).
- Fonseca-Alves, C. E. et al. Current status of canine melanoma diagnosis and therapy: Report from a colloquium on canine melanoma organized by ABROVET (Brazilian Association of Veterinary Oncology). *Front. Vet. Sci.* **8**, 707025. <https://doi.org/10.3389/fvets.2021.707025> (2021).
- Hsieh, R. et al. Mutational status of NRAS and BRAF genes and protein expression analysis in a series of primary oral mucosal melanoma. *Am. J. Dermatopathol.* **39**(2), 104–110. <https://doi.org/10.1097/DAD.0000000000000605> (2017).
- Goodman, A. M. Tumor mutational burden as an independent predictor of response to immunotherapy in diverse cancers. *Mol. Cancer Ther.* **16**, 2598–2608. <https://doi.org/10.1158/1535-7163.MCT-17-0386> (2017).
- Castle, J. C. et al. Exploiting the mutanome for tumor vaccination. *Cancer Res.* **72**, 1081–1091. <https://doi.org/10.1158/0008-5472.CAN-11-3722> (2012).
- Sahin, U. et al. Personalized RNA mutanome vaccines mobilize poly-specific therapeutic immunity against cancer. *Nature.* **547**, 222–226. <https://doi.org/10.1038/nature23003> (2017).
- Grenier, J. M., Yeung, S. T. & Khanna, K. M. Combination immunotherapy: Taking cancer vaccines to the next level. *Front. Immunol.* **9**, 610. <https://doi.org/10.3389/fimmu.2018.00610> (2018).
- McCann, K. et al. Targeting the tumor mutanome for personalized vaccination in a TMB low non-small cell lung cancer. *J. Immunother. Cancer.* **2022**10, e003821. <https://doi.org/10.1136/jitc-2021-003821> (2022).
- Lee, S. Y., Lee, M., Yu, D. S. & Lee, Y. B. Identification of genetic mutations of cutaneous squamous cell carcinoma using whole exome sequencing in non-Caucasian population. *J. Dermatol. Sci.* **106**, 70–77. <https://doi.org/10.1016/j.jdermsci.2022.03.007> (2022).
- Zhao, A. et al. Analysis of genetic alterations in ocular adnexal mucosa-associated lymphoid tissue lymphoma with whole-exome sequencing. *Front. Oncol.* **12**, 817635. <https://doi.org/10.3389/fonc.2022.817635> (2022).

28. Liang, H. et al. Characterization of somatic mutations that affect neoantigens in non-small cell lung cancer. *Front. Immunol.* **12**, 749461. <https://doi.org/10.3389/fimmu.2021.749461> (2022).
29. Moradi, N., Ohadian Moghadam, S. & Heidarzadeh, S. Application of next-generation sequencing in the diagnosis of gastric cancer. *Scand. J. Gastroenterol.* **57**, 842–855. <https://doi.org/10.1080/00365521.2022.2041717> (2022).
30. Hitte, C. et al. Genome-wide analysis of long non-coding RNA profiles in canine oral melanomas. *Genes (Basel)*. **10**, 477. <https://doi.org/10.3390/genes10060477> (2019).
31. Alsaihati, B. A. et al. Canine tumor mutational burden is correlated with TP53 mutation across tumor types and breeds. *Nat. Commun.* **12**, 4670. <https://doi.org/10.1038/s41467-021-24836-9> (2021).
32. Das, S., Idate, R., Cronise, K. E., Gustafson, D. L. & Duval, D. L. Identifying candidate druggable targets in canine cancer cell lines using whole-exome sequencing. *Mol. Cancer Ther.* **18**, 1460–1471. <https://doi.org/10.1158/1535-7163.MCT-18-1346> (2019).
33. Bowlit Blacklock, K. L. et al. Genome-wide analysis of canine oral malignant melanoma metastasis-associated gene expression. *Sci. Rep.* **9**, 6511. <https://doi.org/10.1038/s41598-019-42839-x> (2019).
34. Wang, G., Wu, M., Durham, A. C., Mason, N. J. & Roth, D. B. Canine Oncopanel: A capture-based, NGS platform for evaluating the mutational landscape and detecting putative driver mutations in canine cancers. *Vet. Comp. Oncol.* **20**, 91–101. <https://doi.org/10.1111/vco.12746> (2022).

## Acknowledgements

This study was funded by FAPESP/FAPERGS call, respectively by the Fundação de Amparo à Pesquisa do Estado de São Paulo, FAPESP, Process number 2019/15261-0, and by Fundação de Amparo à Pesquisa do Estado do Rio Grande do Sul, FAPERGS, Process number 19/2551-0002269-7.

## Author contributions

M.L.Z.D., F.K.S. and T.V.C designed the study, acquired funds and wrote the manuscript; C.C.Y, C.O.M, R.H., and S.V.L. provided samples and clinical data, M.K.N., T.L.I., I.I.M.F., F.S.K., C.D.H. and J.V.P.L. performed sample sequencing steps and computational analyses

## Declarations

### Competing interests

The authors declare no competing interests.

## Additional information

**Supplementary Information** The online version contains supplementary material available at <https://doi.org/10.1038/s41598-024-74748-z>.

**Correspondence** and requests for materials should be addressed to M.L.Z.D.

**Reprints and permissions information** is available at [www.nature.com/reprints](http://www.nature.com/reprints).

**Publisher's note** Springer Nature remains neutral with regard to jurisdictional claims in published maps and institutional affiliations.

**Open Access** This article is licensed under a Creative Commons Attribution-NonCommercial-NoDerivatives 4.0 International License, which permits any non-commercial use, sharing, distribution and reproduction in any medium or format, as long as you give appropriate credit to the original author(s) and the source, provide a link to the Creative Commons licence, and indicate if you modified the licensed material. You do not have permission under this licence to share adapted material derived from this article or parts of it. The images or other third party material in this article are included in the article's Creative Commons licence, unless indicated otherwise in a credit line to the material. If material is not included in the article's Creative Commons licence and your intended use is not permitted by statutory regulation or exceeds the permitted use, you will need to obtain permission directly from the copyright holder. To view a copy of this licence, visit <http://creativecommons.org/licenses/by-nc-nd/4.0/>.

© The Author(s) 2024